Sensitivity analysis of nitrogen and carbon cycling in marine sediments

Jan M. Holstein[a,1], Kai W. Wirtz[b]

[a] *Institute for Chemistry and Biology of the Marine Environment (ICBM), University of Oldenburg, P.O. Box 2503, 26111 Oldenburg, Germany*
[b] *Institute for Coastal Research, Ecosystem Modelling Dept., GKSS Research Center, 21502 Geesthacht, Germany*

Abstract

Biogeochemical cycles in coastal sediments encompass numerous interconnected processes and are sensitive to a high number of external forces. Usually a small subset of these factors is considered when developing state-of-the-art models of marine nutrient cycling. This study therefore aims to assess the degree of complexity required in the model to represent the dependency of major biogeochemical fluxes on both intrinsic as well as external factors. For this, a sensitivity analysis (SA) of the generic Integrated Sediment Model (*ISM*) was performed comparing two different model setups: 1) a back barrier tidal flat in the German Wadden Sea and; 2) a deep sea site in the Argentine Basin. Both setups were first calibrated to fit pore water profiles of SO_4^{2+}, NH_4^+ and CH_4. We then employed a new type of SA that evaluates parameter impact rather than targeting variable change.

General structural stability of the model is demonstrated by similar sensitivity patterns of both setups regarding carbon and nitrogen cycling. Mean temperature, organic carbon bio-availability, bacterial adaptation and sediment texture emerge as the most influential parameters of ubiquitous importance. It appears that in coastal settings, transport and sediment mixing and the composition of suspended particles in the bottom water are especially important. The nitrogen cycle displays a high responsiveness to internal feedback mechanisms as well as interdependencies to carbon and metal cycling, which is statistically reflected by sensitivities to $79\,\%$ of all parameters. In contrast, the carbon cycle appears to be mainly controlled by organic matter decay. The SA also pointed to unexpected responses of the sediment system, which are analyzed by further scenario calculations. These, for example, reveal a nonlinear response of nitrification, denitrification and benthic fluxes of NH_4 and NO_3 to changing bioturbation and bioirrigation due to the interactions of different metabolic pathways.

Keywords: Sensitivity; Uncertainty analysis; Sediment; Diagenesis; Bacteria; Wadden Sea

1. Introduction

Both the natural and commercial wealth of many coastal areas are at risk of being lost to forces such as eutrophication and climate change. A particular focal point of land ocean atmosphere interactions at the coastal zone are near-shore sediments, which host major biogeochemical cycles relevant to not only regional ecosystems but also the global climate system. Benthic cycles of carbon and nitrogen have the potential to strongly affect the trophic status of the overlying water as well as the release or destruction of greenhouse gases. However, a multitude of processes interact during the benthic turnover of carbon and nitrogen that undermine simple cause effect relationships. Hence, system understanding is a prerequisite for the careful assessment of changes in coastal elementary cycles.

Models can, in principle, provide a holistic representation of benthic biogeochemistry. The endeavor to understand the impact of environmental change to the carbon and nitrogen cycles in coastal sediment demands highly integrated models. High spatiotemporal variability in external forces [41], transport processes (such as physical and biological sediment mixing), bioirrigation, advection [35, 4], and a large number of chemical conversions that are mediated by microbial populations [49] are constitutive elements of many coastal environments. However, most state-of-the-art biogeochemical sediment models fall short for they are constructed for environs that range from continental shelf to deep sea marine sediments [e.g. 21, 50, 53, 46, 54]. Many assume steady state. Usually, the processes that may be relevant in highly dynamic and heterogeneous near-shore systems are only partly integrated.

One major constraint for integrating more processes into models is the lack of observations that can be used for parameterization or validation. Poorly identifiable or non-identifiable model parameters are a well known problem of overparameterized models. However, theoretical studies on the impact of internal feed back mechanisms on biogeochemical cycling can still be conducted even when data are scarce. Constructed to this purpose, the Integrated Sed-

iment Model (*ISM*) is characterized by a high degree of genericity and integration [56]. The *ISM* generates redox zoning through microbial competition with emphasis on reactions related to carbon, nitrogen and metal cycling. Its elevated process and spatial resolution is adapted to the high vertical, lateral and temporal gradients found in chemical inventories of coastal sediments.

The downside of integrating an increasing number of processes into a model is that the numerous interdependencies, together with the nonlinearity of many of the processes, inhibit an *a priori* understanding of the model system. This lack of inferable knowledge is due to the unknown relevance of particular parameters, such as specific process coefficients, that cannot easily be measured accurately and whose level of uncertainty varies depending on the parameter. The model output uncertainty increases as the complexity and number of parameters of uncertain impact and value increase. Compared to parsimonious models, the predictive power is expected to be rather low [51]. It is common sense that offshore environments can be approximated by a classical steady state approach in most instances. This may not be applicable for many aspects of coastal systems. A forced permanency of otherwise transient conditions can become a major obstacle for model validation if the system is rather sensitive to starting conditions or field data are sparse.

Our major motivation in using a highly complex model is to put more emphasis on important indirect processes that are rarely included, such as the microbial control of redox reactions and competition between different chemical pathways. The choice for complexity comes at the cost of constraint. A systematic analysis of the model will reveal which processes are truly connected to carbon and nitrogen cycling and can delineate which are parameters of major impact and which are parameters of minor impact, even though uncertainties remain. This information will facilitate the determination of an optimized level of complexity for biogeochemical models of coastal sediments.

Automated model analysis methods, such as sensitivity analysis (SA), reveal both counter-intuitive model behavior and feedbacks in the model. Discriminating between unexpected and undesired model behavior by subsequent model analysis can be turned into knowledge of the system. By evaluating the impact of parameters on specific processes, SA is a tool to cope with uncertainty [32]. By combining SA and information on parameter uncertainty, the crucial parameters for specific processes can be systematically identified. More robust model results can efficiently be obtained by constraining just the influential parameters of high uncertainty. Alternatively, the respective processes may be revised.

In this study, key parameters for the biogeochemical cycles of carbon and nitrogen in coastal systems are identified by means of a SA applied to the *ISM*, calibrated for a tidal flat. Parameters that are of specific importance to coastal systems are identified by comparison of SA results to those for a deep sea setup, with adjusted parameteriza-

tion. The systematic analyses of the sensitivity of specific output variables to variations of single parameters of the *ISM* provide a look up table for the interdependencies of model dynamics concerning carbon and nitrogen cycling. The supposed nonlinear system behavior is assessed by an elaborate SA method using a newly introduced methodology that acknowledges the large range of uncertainty in many process parameters.

2. Short model description

The *ISM* [56] is a complex sediment model designed to investigate biogeochemical cycles in near-shore sediments employing 55 state variables and 84 parameters. The *ISM* describes transport and reaction of solid and dissolved chemical and biological species in porous aquatic media according to Eq. 1 and was verified in studies of Beck et al. [7, 8]. Spatial discretization is attained using finite boxes. A box-volume is assigned to each node according to simple geometrical calculations and the flux itself is approximated by finite differences. The model is generic in the sense that it captures a large number of potentially relevant mechanisms, including advection, bioturbation, bioirrigation, erosion and sedimentation. In contrast to most other diagenetic models, the *ISM* resolves organic matter (OM) degradation in greater detail, in particular the OM catabolism that is mediated by both heterotrophic and lithotrophic microbes as depicted in Fig. 2. Chemical conversions primarily depend on microbial population dynamics driven by physical forcing, transport and nutrition. The microbes are subdivided into 20 functional groups according to their metabolic redox path listed in Tab. 2. Analogous to the Gibbs free energy of these conversions, the energy yield of the bacterial catabolism is specific to the different functional groups and affects the competitive position of the microbe. Extending the original model of Wirtz [56], model boxes may have different porosities, chemical species have specific molecular diffusion coefficients and bacteria can switch to dormancy when undersupplied. A more complete description of the *ISM* is given in Appendix A.

3. Sensitivity analysis

A sensitivity analysis (SA) can be used to enhance understanding of a model system by quantifying and visualizing cause-and-effect relationships. Related to optimization problems often encountered in traditional model calibration tasks, an SA estimates the contribution of parameter uncertainty to model output, thus providing information about the relevance of the represented processes for the overall system dynamics. A SA will yield details on the sensitivity of model dynamics to the parameters. In this manner, an SA provides knowledge essential for a wide range of model applications: planning field studies to

Species conc.   Diffusion/Dispersion/Bioturbation   Reactions

$$\phi_p \frac{\partial C_i}{\partial t} = \sum_{r=x,z} \left(-\frac{\partial \phi_p \mathrm{v} C_i}{\partial r} + \frac{\partial}{\partial r}\left(\phi_p D_i \frac{\partial C_i}{\partial r} \right) \right) + \phi_p \beta_z (C_{0,i} - C_i) + \phi_p \sum_{j=1}^{M} s_{i,j} R_j(C_1, \cdots, C_N) \quad (1)$$

Advection/Sedimentation   Bioirrigation

Figure 1: With i=1, ...,N, index of chemical species (N=15); j=1, ...,M, index of reactions (M=34); t, r, independent variables: time and space; r, spatial direction; can be x (horizontal) or z (vertical); C_i, concentration of ith species; $C_{0,i}$, bottom water concentration of ith species; ϕ_p, porosity (ϕ) for solutes or $(1-\phi)$ for solids; v, sedimentation rate or macroscopic ow velocity; D_i, diffusion and bioturbation coefcient of ith species species; β_z, bioirrigation coefcient; R_j, rate of jth reaction; $s_{i,j}$, stoichiometric coefficient for i^{th} species in j^{th} reaction.
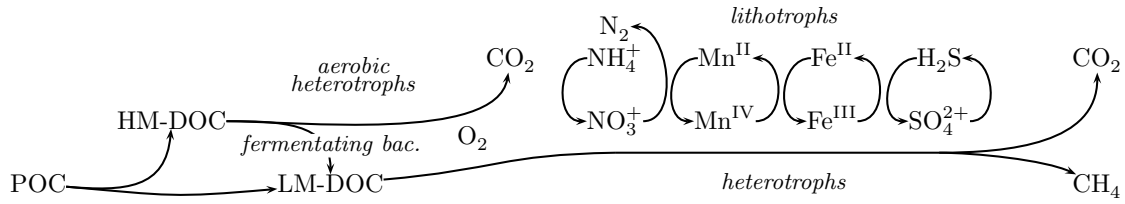

Figure 2: Sketch of the organic carbon degradation scheme. Positions of functional groups of bacteria therein and the lithotrophic OM oxidant regeneration cascade are roughly outlined. The quality class subdivision of POC, high- and low-molecular DOC (HM- and LM-DOC) is not shown.

assess critical parameters [32], refinement of critical processes, or general model development, adaptation and reduction [45]. SA is related to identifiability analyses which aims to assess if or to what extent parameters are uniquely determined. For small models (in the sense that they have few parameters), the parameter identifiability problem can be approached by a graphical analysis of sensitivities in order to analyze parameter interdependencies [28, 31]. Based on local sensitivity analysis, Brun et al. [17] developed an formal identifiability analyses technique for large models that Andersson et al. [3] applied on a bioirrigation model in order to assess different sampling strategies regarding their efficiency to constrain a small subset of parameters. It is accepted that sediment biogeochemical model studies at least need to assess the sensitivity of major target variables. Soetaert et al. [46] examined changes to the carbon mineralized in their large early diagenesis model due to one-at-a-time variation of selected variables. Berg et al. [11] introduces a sensitivity measure to assess the impact of a one-at-a-time 5 % change in selected variables to 2 target variables. Superior to linear SA are efforts to calculate the local 2nd partial derivatives in order to factor nonlinearities in Dale et al. [19].

The initial step of an SA is the definition of target variables. The selection of variables should align with the research question. As such, the set of target variables, which are usually state variables or functions thereof, can be very confined, with the goal of testing one or few specific processes, or broadly diversified, in order to represent major model dynamics.

The standard way of performing an SA is to alternately increase and decrease a parameter P of interest (standard setting is P_0) by the amount $v \cdot P_0$. The resulting values of the target variable T, T_{v+} and T_{v-} are compared with the value at standard parameterization T_R. The sensitivity $\mathcal{S}_v(T)$ is then defined as

$$\mathcal{S}_v(T) = \mbox{\small 1/2} \left| \frac{T_R - T_{v+}}{T_R} \right| + \mbox{\small 1/2} \left| \frac{T_R - T_{v-}}{T_R} \right| \qquad (2)$$

The commonly used index $\mathcal{S}$ is a property of a given target variable and critically depends on v. The soundness of the sensitivity measure depends on the parity between the natural heterogeneity of the parameter uncertainties and the respective choices of v. This can be avoided by defining the quantity leverage $\mathcal{L}_T(P)$ of P with regard to T, which is a property of a given parameter and measure for the magnitude of v corresponding to a predefined sensitivity $\mathcal{S}^*$ (here $\mathcal{S}^*$ = 0.05), i.e. a 5 % target variable change

$$\mathcal{L}_T(P) \stackrel{\mathrm{def}}{=} -\log|v|, \quad \mbox{for} \ \ \mathcal{S}_v(T) \geq \mathcal{S}^*, \qquad (3)$$

Assuming continuity of $\mathcal{S}_v(T)$, $\mathcal{L}_T(P)$ is estimated by perpetual execution of the simulation in which the parameter is systematically varied, a procedure referred to as parameter variation. The parameter variation is controlled by v, which starts at a small value and is subsequently increased. When $\mathcal{S}_v(T)$ exceeds or equals $\mathcal{S}^*$, $\mathcal{L}_T(P)$ is found. Since $\mathcal{L}$ is the negative logarithm of the relative parameter change, greater leverages stand for higher sensitivity of T with respect to P. For the application to the *ISM*, the initial v was set to 0.001 (corresponding to a parameter change of 0.1 %) and an upper limit of

3

$v_{max} = 1000$ was imposed, allowing for an evaluation of target variable sensitivity within 7 magnitudes of parameter range, i.e. $3 \geq \mathcal{L} \geq$ -3. If parameters are only valid on a restricted scale, e.g. $0 > P > 1$, insensitivity may already be ascertained from values well below v_{max}. It should be noted, that due to the iteration scheme, calculating leverages leads to higher numerical effort.

4. Model setups, reference data and variables of interest

The model setup for coastal conditions was calibrated to reproduce the vertical pore water profiles of SO_4, NH_4 and CH_4 and bacterial abundance using an automated Monte-Carlo technique. From preliminary sensitivity studies, a set of parameters was identified that mainly control organic matter hydrolization, sulfate reduction, methanogenesis and AMO. In subsequent simulations, these parameters are set to random values within reasonable limits. The parameter set from which the empirical data are reproduced best in terms of integrated square root mean error was used as tidal flat calibration. We checked whether calibrated parameter values converge towards unique values. The model setup for deep sea conditions is based on the tidal flat calibration. The differences to the tidal flat setup regards boundary conditions like bottom water concentrations, temperature, absence of tides, and difference in sediment permeability. According to the valid assumption, that organic matter is less reactive and that sediment mixing (bioturbation) and pumping (bioirrigation) is less pronounced at the deep sea site, the related parameters are adjusted appropriately.

The model setups for coastal and deep sea conditions were calibrated using vertical pore water profiles of SO_4, NH_4 and CH_4 and bacterial abundance (for the tidal flat setup) data representative of either a typical sandy tidal flat in the back barrier area of the German Wadden Sea (53° 43.270' N, 7° 43.718' E) [29, 55] or the deep sea site GeoB 6229, located in 3443 m water depth at the continental slope to the Argentine Basin in the South Atlantic (37° 12.41' S, 52° 39.01' W [44]), respectively. The agreement between model results and data shown in Fig. 3 is very good for both sites, though the coexistence of SO_4 and CH_4 in the upper part of the tidal flat site could not be reproduced. In both setups oxygen penetration turned out to be low or very low (mm to few cm) and sulfate-methane interfaces are generated, dominated by sulfate reduction at the tidal flat site and by anaerobic methane oxidation at the deep sea site. The model calibration generated two sets of parameter values. The parametrization differences are summarized in Tab. 1.

Generally, tidal flat sediments are characterized by a high content of labile OM and high activity of bioturbating and bioirrigating organisms. Daily as well as seasonal variability are pronounced due to tidal forcing and shifts in temperature and in the concentrations of many chemical species within the bottom water. In contrast, boundary conditions in the deep sea site remain constant, except slight annual temperature variations. OM content of the surface sediment (0.5 cm) is higher than at the tidal flat site, but the material is mostly refractory.

This study aims to achieve a relatively complete assessment of factors controlling the N and C cycling in marine sediments, therefore, nine target variables where selected to represent model dynamics. In order to manage the total number of target variables, we choose to aggregate the carbon and nitrogen that is processed by each of the specific reaction pathways into Shannon Wiener Indices [e.g. 9]. The Shannon Wiener Index of diversity (SWID) is a measure of how a reactant is distributed among different reaction pathways. Changes in the indices SWID-OM and SWID-NO3 are calculated from the spatiotemporal mean rates of reactions R-10 through R-15 and R-11, R-17, R-31, R-33 and R-54, respectively (reactions according to Tab. 2). Shifts in the dominance structure of carbon and nitrogen pathways are indicated by changes in the respective SWID. The SWID is calculated from the number of different pathways G and the amount of substrate consumed f_i by the ith pathway, $SWID = \sum_{i=1}^{G} f_i/F \cdot \ln(f_i/F)$, with $F = \sum_{i=1}^{G} f_i$. The spatiotemporal mean rates of CO_2 and CH_4 production actually account the totals of both carbon turnover and the gross activity of the heterotrophic functional groups. Likewise, spatiotemporal mean rates of nitrification and denitrification cover the large part of nitrogen turnover and the gross activity of the nitrogen functional groups. The average benthic fluxes of CH_4, NO_3 and NH_4 serve as further indicators for sediment geochemistry. In a final stage of the SA, a more detailed analysis of how either influential or unconstrained parameters affect nitrogen dynamics is carried out by a continuous variation of such model coefficients.

5. Results

5.1. Sensitivity analysis

The SA reveals the ubiquitous relevance of temperature, transport and sediment mixing, organic matter composition, and bacterial metabolism for carbon and nitrogen cycles. In contrast, bottom water concentrations and individual reaction specific coefficients (biotic and abiotic) have marginal impact, as shown in Fig. 4. In Fig. 4 the complicated patterns of model sensitivities are summarized and leverages in each sub-categories are shown as aggregated into a single average value regarding carbon or nitrogen specific target variables. The structural stability and therefore robustness of the model dynamics is reflected by the similarity of the general sensitivity pattern of the tidal flat and deep sea setups, as seen in Fig. 5. The parameter sub-categories are given on the left.

Temperature is the most influential parameter. Abiotic reactions, microbial growth, OM decay and molecular diffusion are affected by temperature. In addition, parameters controlling porosity, the decomposition and quality
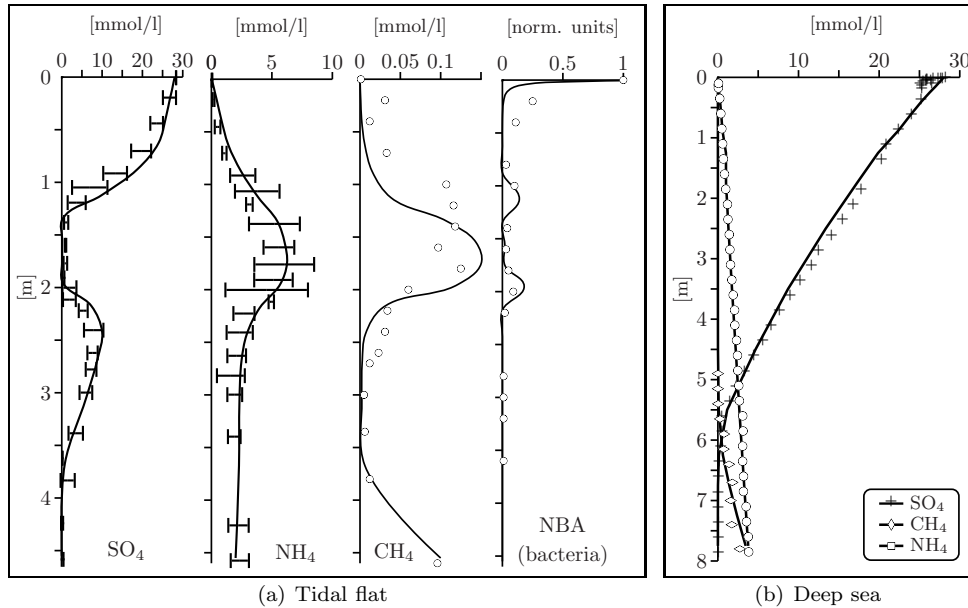
Figure 3: Data and model results for sulfate, ammonium, methane and normalized bacterial abundances (NBA) for two sites. Error bars represent standard deviation from parallel cores. (a) Tidal flat - pore water profiles from Neuharlingersieler Nacken [55]. (b) Deep sea - Station GeoB 6229 in the Argentine Basin, 3443 m water depth [44]. Note the different z-axis scales.

Table 1: Calibrated parameter and boundary values differing between the tidal flat and the deep sea setup.

Parameter	Symbol	Setup A (tidal flat)	Setup B (deep sea)	unit
tidal cycle length	τ	0.53	∞	d
exposure during low tide	γ	0.5	0	d/d
bioirrigation coefficient	β	6.0	0.02	1/d
bioturbation coefficient	D^B	0.2	0.05	cm^2/d
porosity	ϕ	0.65 - 0.35	0.9 - 0.65	cm^3/cm^3
high quality POC decay rate	λ_0	1.2×10^{-2}	4.2×10^{-3}	1/d
medium quality POC decay rate	λ_1	1.0×10^{-4}	1.2×10^{-5}	1/d
low quality POC decay rate	λ_2	1.0×10^{-5}	1.0×10^{-6}	1/d
temperature amplitude	ΔT	21.6	0.5	$^\circ$C
O_2 bottom water concentration	BW_{O2}	0.35 - 0.20[†]	0.2	mmol/l
NH_4 bottom water concentration	BW_{NH4}	0.01 - 0.02[†]	0.03	mmol/l
NO_3 bottom water concentration	BW_{NO3}	0.015 - 0.0015[†]	0.03	mmol/l
DOC bottom water concentration	BW_{DOC}	0.4	0.135	mmol/l
POC bottom water concentration	BW_{POC}	0.1 - 0.6[†]	0.001	mmol/l

[†] changes within a seasonal cycle.

of OM, and the growth and turnover rates of bacteria have universal character and strong leverage. Variation in these parameters generates responses in the majority of the target variables regardless of the setup. The tidal flat setup does appear to be more sensitive to parameter changes throughout all categories, with average changes of 0.6 leverage units. The higher sensitivity of the tidal flat setup is most striking in the parameter sub-categories for transport and mixing, organic matter, and global bacterial parameters. External tidal forces, which are not active in the deep sea setup, also significantly affect all target variables. Parameters related to bioturbation and bioirrigation show medium leverages for the tidal flat setup and low leverages for the deep sea setup. The transport and mixing parameters are clearly influential on nitrogen cycling outputs, but have mediocre leverage on carbon cycling. Of all parameters tested, transport and mixing are the least similar in relation to nitrogen and carbon cycling

outputs for both tidal flat and deep sea conditions.
Responses to changing bacterial yield constants (reaction specific energy yields) are more heterogeneous, reflecting the relative importance of the reactions in terms of carbon and nitrogen turnover, e.g. the domination of the tidal setup by sulfate reduction versus the importance of oxic and suboxic reactions in the deep sea setup.
In the tidal setup, a statistical analysis of the leverage classes reveals that insensitivity occurred in about 50 % of all cases, as indicated by leverages of -3. However, given a total of 84 parameters, the chosen target variables are sensitive to 40 parameters on average (leverage above -1). Only 7 parameters have no effect on any of the target variables; these parameters are consistently unrelated to C and N cycling and therefore not covered by the target variables. Within the set of the leverages above -3, leverage class 0 (a parameter change of less than one magnitude is required for a significant system reaction ($\mathcal{S}^*$)), forms

Symbol

Description

Temp.

T_R — reference temperature

Transport & mixing

τ — tidal cycle length
γ — athmospheric exposure during low tide
— diffusion enhancement
β — bioirrigaton coefficient
z_β — bioirrigaton depth
D^B — bioturbation coefficient
z_B — bioturbation depth
— benthic boundary layer thickness
ϕ — porosity

Organic matter

q_{DOC} — global DOC quality constant
λ — global POC decay constant
— enzymatic enhancment of POC decay
— quota of POC allocation to DOC quality class
— fractal dimension of POC surface
— N content of OM

Global bacterial parameters

r_g — bacterial uptake rate
σ — bacterial growth rate
m — bacterial mortality
δ — dormancy effect on respiration
$\mathcal{Q}_{10}$ — Temperature susceptibility of bacterial metabolism
a_{max} — maximum quota of bacteria sticking to solids
a_{min} — minimum quota of bacteria sticking to solids
α_{max} — maximum quota of active bacteria
α_{min} — minimum quota of active bacteria
X_{cap} — carrying capacity for bacteria
— minimum bacterial population

Reaction specific energy yields

fermentation yield (R-1)
O_2 reduction yield (R-10)
NO_3 reduction yield (R-11)
MnO_2 reduction yield (R-12)
$Fe(OH)_3$ reduction yield (R-13)
SO_4 reduction yield (R-14)
Methanogenesis yield (R-15)
aerob NH_4 reduction yield (R-16)
anaerob NH_4 reduction yield (R-17)
anaerob NH_4 reduction yield with MnO_2 (R-18)
Mn^{II} oxidation yield with O_2 (R-30)
Mn^{II} oxidation yield with NO_3 (R-31)
Fe^{II} oxidation yield with O_2 (R-32)
Fe^{II} oxidation yield with NO_3 (R-33)
Fe^{II} oxidation yield with $VMnIV$ (R-34)
H_2S oxidation yield with O_2 (R-35)
H_2S oxidation yield with Mn^{IV} (R-36)
H_2S oxidation yield with Fe^{III} (R-37)
CH_4 oxidation yield with O_2 (R-37)
CH_4 oxidation yield with SO_4 (R-38)

Column labels (both setups):
SWI-OM, CO2 production, CH4 production, benthic CH4 flux, SWI-NO3, benthic NO3 flux, benthic NH4 flux, Nitrification, Denitrification

Leverage $\mathcal{L}$
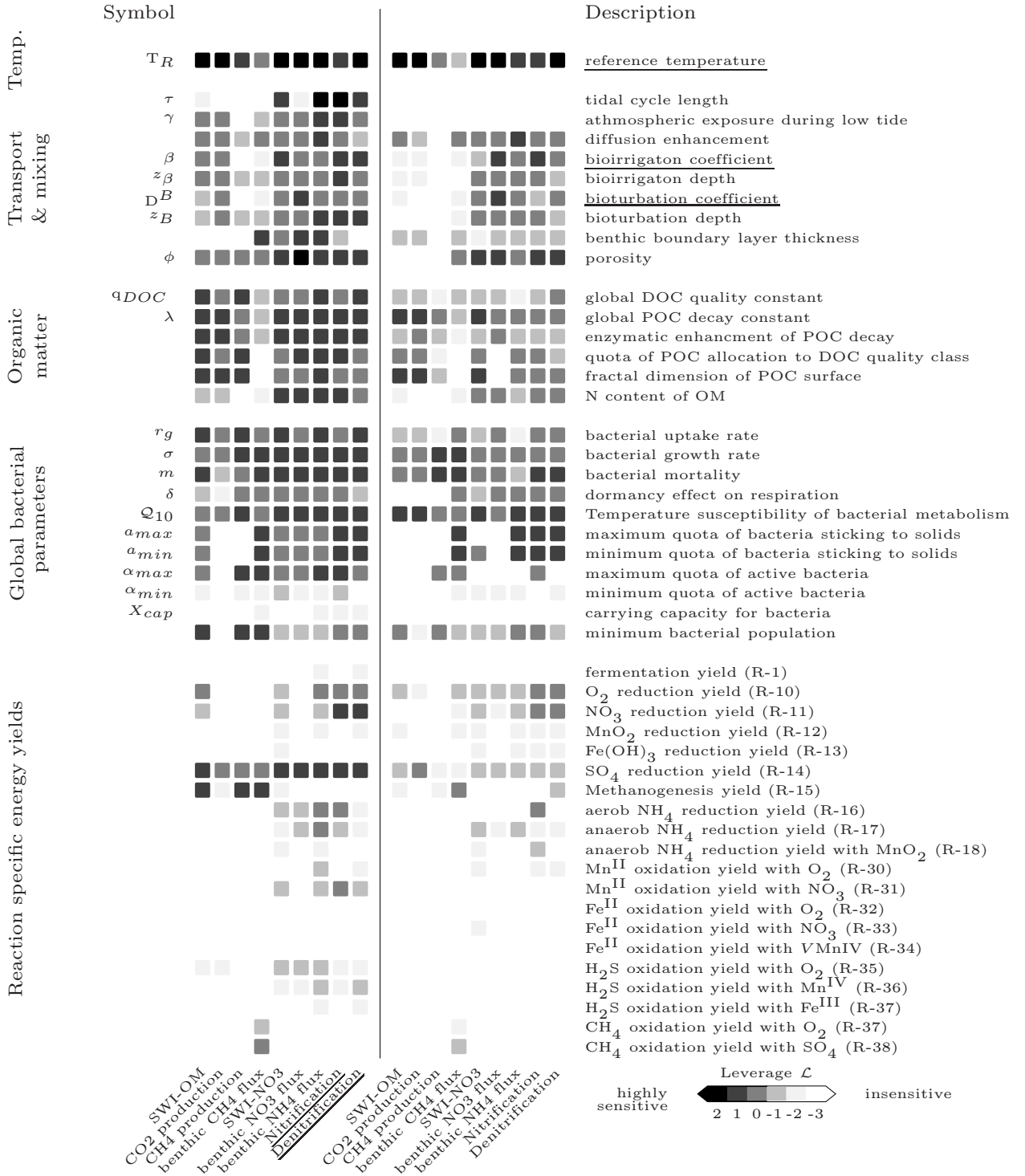
highly sensitive — 2 1 0 -1 -2 -3 — insensitive

Figure 5: Comparison of sensitivity matrices of setup A (Wadden Sea) and setup B (deep sea). Shading intensity corresponds to the leverage of parameters, i.e. dark shading indicates that rather small parameter changes are sufficient to produce a predefined change in the respective target variable. Parameters and target variables that were further investigated with scenario analyses are underlined. Parameters denoted as symbols are defined in the Appendix. The parameters have been divided into 7 subsets by relation to the process they reflect as shown on the left of the figure.
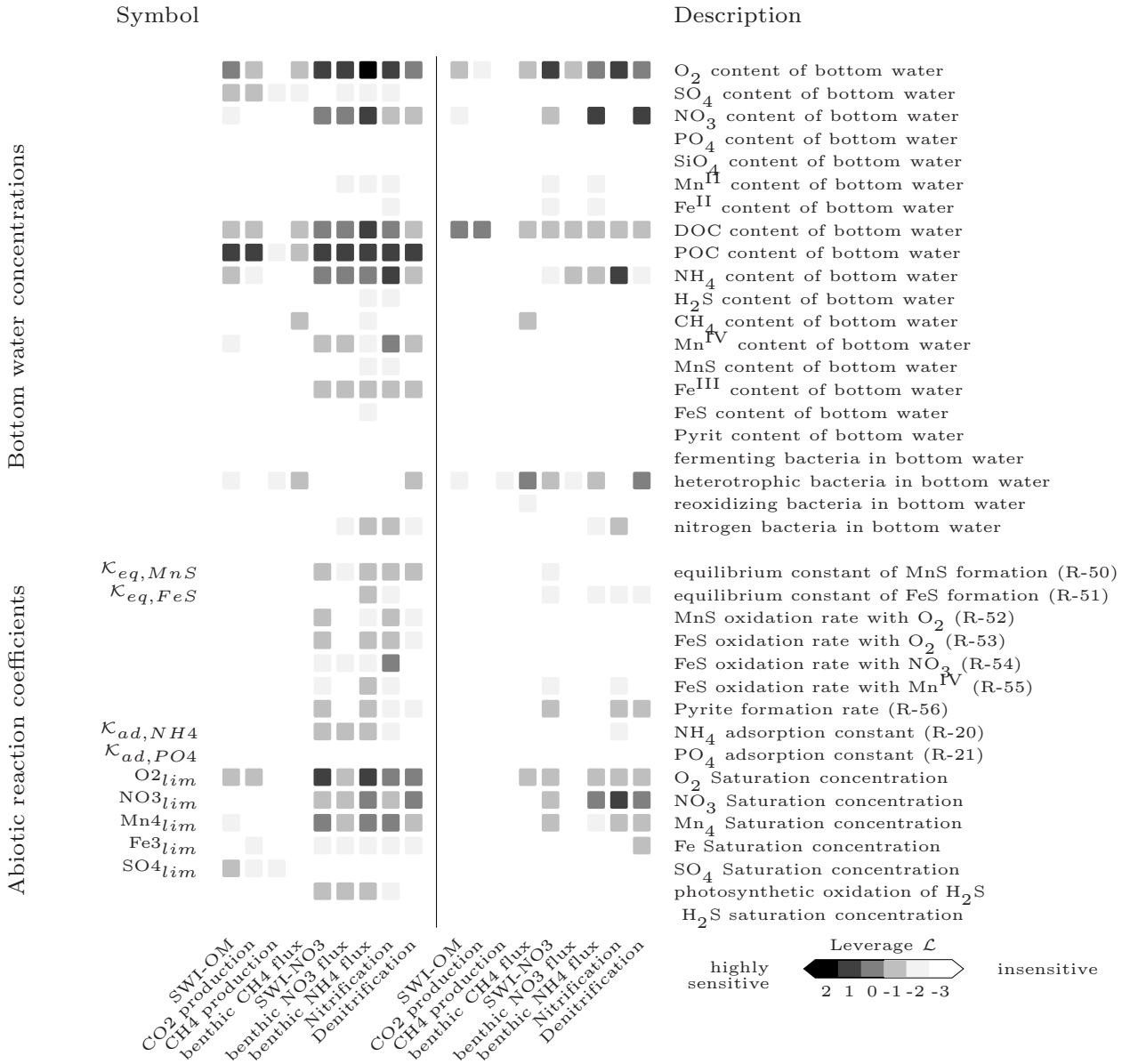
Tidal flat setup Deep sea setup

Symbol   Description

Bottom water concentrations

O_2 content of bottom water
SO_4 content of bottom water
NO_3 content of bottom water
PO_4 content of bottom water
SiO_4 content of bottom water
Mn^{II} content of bottom water
Fe^{II} content of bottom water
DOC content of bottom water
POC content of bottom water
NH_4 content of bottom water
H_2S content of bottom water
CH_4 content of bottom water
Mn^{IV} content of bottom water
MnS content of bottom water
Fe^{III} content of bottom water
FeS content of bottom water
Pyrit content of bottom water
fermenting bacteria in bottom water
heterotrophic bacteria in bottom water
reoxidizing bacteria in bottom water
nitrogen bacteria in bottom water

Abiotic reaction coefficients

$\mathcal{K}_{eq,MnS}$ equilibrium constant of MnS formation (R-50)
$\mathcal{K}_{eq,FeS}$ equilibrium constant of FeS formation (R-51)
                          MnS oxidation rate with O_2 (R-52)
                          FeS oxidation rate with O_2 (R-53)
                          FeS oxidation rate with NO_3 (R-54)
                          FeS oxidation rate with Mn^{IV} (R-55)
                          Pyrite formation rate (R-56)
$\mathcal{K}_{ad,NH4}$ NH_4 adsorption constant (R-20)
$\mathcal{K}_{ad,PO4}$ PO_4 adsorption constant (R-21)
$O2_{lim}$ O_2 Saturation concentration
$NO3_{lim}$ NO_3 Saturation concentration
$Mn4_{lim}$ Mn_4 Saturation concentration
$Fe3_{lim}$ Fe Saturation concentration
$SO4_{lim}$ SO_4 Saturation concentration
                          photosynthetic oxidation of H_2S
                          H_2S saturation concentration

SWI-OM
CO2 production
CH4 production
benthic CH4 flux
SWI-NO3
benthic NO3 flux
benthic NH4 flux
Nitrification
Denitrification

SWI-OM
CO2 production
CH4 production
benthic CH4 flux
SWI-NO3
benthic NO3 flux
benthic NH4 flux
Nitrification
Denitrification

Leverage $\mathcal{L}$

highly
sensitive   insensitive
           2 1 0 -1 -2 -3

Figure 5: continued...

the largest group, accounting for nearly a third of all cases. The classes -1 and -2 (parameters that have milder effects) and class 1 (parameters that have greater impacts) each constitute about one-fifth of the effective leverages.

Nitrogen-related target variables display a higher sensitivity compared to carbon cycle-specific variables. This difference is most pronounced for transport and mixing parameters, which have nearly no effect for deep sea carbon cycling. The high N-cycling responsiveness is reflected by the sensitivities of the five nitrogen-related target variables, which exceed those of the carbon-related target variables in terms of average sensitivity and number of influential parameters. For example, when counting leverage -1 and up, the benthic NO_3 flux, SWID-NO3 and nitrification are each sensitive to changes in more than 40 parameters. In contrast, methanogenesis is sensitive to only a very few, but highly influential, parameters. According to the numbers of influential parameters, CH_4, and especially its production, and the DOC partitioning are characterized as less interrelated indicators with an intermediate mean effective leverage of a little less than zero. The stimulating effect of redox environment oscillation created by variable tidal current and recurrent atmospheric exposure is documented by the high leverage of the tidal cycle length. Although the tidal cycle frequency is fixed and completely constrained, redox oscillation can also occur in the field through bioturbation by relocating sediment into a different redox environment [1]. While nitrogen cycling is very sensitive to redox oscillation, the carbon turnover seems unaffected.

The carbon cycle responds in a linear way to changing model coefficients. Highly influential parameters for CO_2 generation capacity are rare and exclusively relate directly to POC decay. The low impact of reaction specific energy yields and bottom water concentrations add to the picture of a predominantly electron donor-limited system.
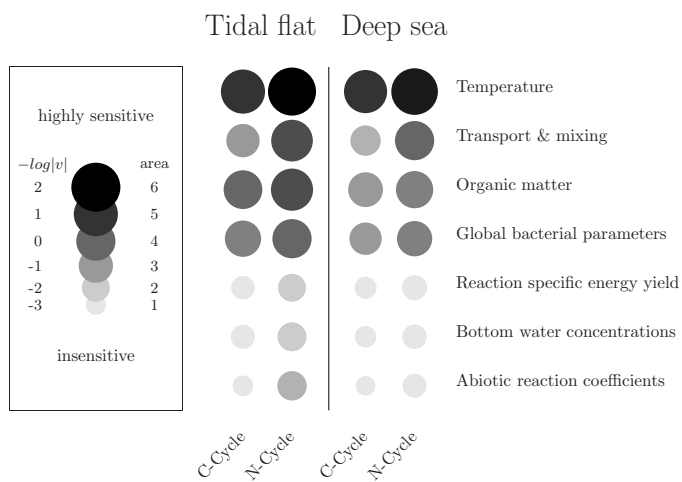
Figure 4: Condensed view of the sensitivities of the carbon and nitrogen cycles with regard to different parameter subsets for the tidal flat and deep sea setups. Area and shading represent leverage, e.g. leverage 0 is displayed with four times the area of leverage -3.

The general congruence of the leverage patterns of CO_2 and the SWID-OM suggests the predominance of a coherent carbon degradation scheme. Thus, shifts in the partitioning of DOC consumption pathways are not predominantly due to competition. The rare cases in which functional groups of bacteria increase in dominance at the expense of other groups usually involve a change in a parameter that directly relates to the competitiveness of the functional group, the reaction specific energy yield. For example, the methanogenesis yield reflects the potential of methanogens to indirectly compete with sulfate reducers by up and down movement of the sulfate methane interface. Also, a variation in the oxygen reduction yield is, in large part, compensated for by subsequent pathways (NO_3, Mn, etc.). Apart from functional group-specific parameters, global regulatory parameters for bacterial survival and proliferation also affect the competitive success of heterotrophic functional groups e.g. bacterial mortality. The nitrogen cycle displays an inhomogeneous pattern of sensitivity to changes in input parameters. Organic matter and coefficients for bacterial population growth have a relatively uniform impact, but transport and mixing parameters appear asymmetric in their effect on nitrogen cycling. None of the input parameters has the same leverage on all nitrogen target variables and no two parameters have the same leverage pattern. Additionally, the leverage pattern of the tidal flat and the deep sea setup differ considerably. The variable responses of the nitrogen cycle to changes of transport and mixing parameters reflect different feedbacks of the nitrification / denitrification cascade and partial decoupling from carbon cycling, even in the monotonous deep sea environment. In all, the deep sea nitrogen cycle seems less affected by changes of global bacterial parameters, especially regarding bacterial uptake, growth, and mortality, which have less leverage on both the N-specific conversion rates and the SWID-NO3. In opposition to the general trend, bacterial adhesion, dormancy, and temperature susceptibility of bacteria active in nitrogen metabolism mostly gain in relevance in the monotonous and less prosperous environmental conditions of the deep sea setup.

In summary, when the model is calibrated for a tidal flat setting, it shows higher sensitivity to changes in the input parameters than when it is run in the deep sea setup, both with respect to average sensitivity and the number of parameters with high leverage. However, the two setups show a comparable sensitivity pattern. Key parameters are reference temperature, temperature coefficient Q_{10}, microbial growth rate, POC decay rate, and porosity. This emphasizes the universal importance of external temperature forcing, bacterial adaptation, and sediment texture for diagenesis. The nitrogen cycle appears to be linked to a high number of model processes and all associated target variables depend on a notably large number of parameters with mostly medium leverage. The carbon cycle associated target variables, on average, have lower responsiveness and less dependencies. For example, the methane

cycle is sensitive only to few parameters that have high leverages.

5.2. Scenario analyses

Model analysis reveals that essential parts of the tidal flat nitrogen cycle, namely nitrification, denitrification and efflux of NH_4 and NO_3, are dependent on bioirrigation and bioturbation in a nonlinear way. Temperature, albeit the most influential parameter, has a rather unspecific and more linear impact.

The similar dependencies of nitrification and denitrification on bioirrigation are depicted in Fig. 6. A bioirrigation coefficient of approx. $1 \, d^{-1}$ marks the turning point where enough oxygen is pumped into the sediment for nitrifiers to successfully compete with sulfide oxidizers. Here, the sediment shifts from importing to exporting NO_3. This is also expressed by the leveling-off of the benthic ammonium flux when the bioirrigation coefficient exceeds $1 \, d^{-1}$, as illustrated in Fig. 7. Bioturbation has a different effect on nitrification. Below approx. $2 \, cm^2/d$, nitrifiers benefit from ammonium imported from deeper zones where sulfate reducers efficiently enhance OM degradation and ammonium release. At higher bioturbation rates, large quantities of surficial OM are transported to anoxic depths, leading to enhanced sulfide generation and sulfide oxidizers are increasingly outcompeting nitrifiers, and thus inhibiting nitrification. At very high bioturbation rates, denitrification surpasses nitrification, leading to a net NO_3 import. Denitrification decreases with increasing bioturbation due to OM export from suboxic layers. The impact of temperature on nitrification is lower than on denitrification. Since T_R is the reference temperature for the rate-modifying temperature function, a raise in T_R emulates a decline in environmental temperature and vice versa, illustrated in Fig. 6 and Fig. 7. Nitrifiers are usually oxygen-limited, hence, they do not benefit from a temperature-related increase of POC decay and subsequent ammonium release. The effect of temperature-regulated metabolic activity on ammonium conversion rates is partly compensated by increased upward diffusion of reduced chemical species like Mn^{2+} or H_2S at higher temperatures due to enhanced activity of anaerobic or lithotrophic bacteria. The increased share of oxygen consumed by the reoxidation of reduced inorganic species exerts competitive stress on nitrifiers and inhibits a significant rate increase at reference temperatures below 293 K. Consequently, NO_3 production remains low at elevated temperatures and denitrifiers are outcompeted by sulfate reducers. The benthic nitrate flux decreases with lowered reference temperature accordingly.

6. Discussion

The leverage table in Fig. 5 provides a holistic view of the interrelationships within the simulated biogeochemical systems. Generally, sensitivities do not contradict sensible expectations, e.g. the dependence of benthic O_2 flux on the O_2 bottom water concentration. Confirming the results of Andersson et al. [3], who compared a model setting for shallow conditions with one for deep sea regarding parameter identifiability, it is found that the inherent model dynamics, expressed by the leverage patterns, is substantially similar despite the contrasting parameter settings between tidal flat and deep sea. In accordance to other modelling studies, we identified a few key parameters that, when slightly changed, lead to drastic variations in the model output. One such parameter is organic carbon bio-availability, which largely controls early diagenetic transformations and is, thus, expected to be of great importance [40]. The high relevance of transport, sediment mixing and porosity parameters was already shown by Andersson et al. [3] and Berg et al. [10]. Berg et al. [11] also found that organic matter reactivity is one of the most influential parameters. Although temperature is the most influential parameter, it's normally high level of certainty prevents that temperature is included in diagenetic model sensitivity studies. It is demonstrated by high ubiquitous impact of temperature and the scenarios in 5.2 that temperature must not be neglected, specifically in highly variable environments where temperature uncertainty may be quite considerable. Bacterial metabolism is rarely included into diagenesis models and therefore sensitivity data on bacterial parameters are scarce. The high impact of bacterial parameters on carbon and nitrogen cycling challenges the common approach of including bacterial concerns into reaction coefficients.

The information compiled in the sensitivity table can be used to characterize the biogeochemical mode of the modeled system (such as the SO_4 domination of the tidal flat setup or the oxic/suboxic dominance in the deep sea setup) and to isolate influential processes for specific model outputs. In addition, the use of the model to constrain parameters is limited to parameters with high leverages. Constraints by model calibration of less influential parameters like most of the reaction specific energy yields or the abiotic reaction coefficients may be tainted with great uncertainty. The SA helps to identify unrealistic parameterizations as well as problematic or unessential model formulations. For example, the carrying capacity for bacteria, which should reduce bacterial growth at high numbers due to spatial limitations, appears ineffective in both setups. Further investigation revealed that false parameterization caused the failed effect. Though efforts to independently constrain parameters cannot be replaced by SA, parameters commonly cannot be constrained as desired specifically if parameters are not physical quantities like the carrying capacity. In these cases the SA is helpful to identify the parameter leverages, for instance, to increase the efficiency of automated fitting or skipping unnecessary processes. It was also revealed by the SA that the model concept of a minimum starting bacterial population, which allows bacteria a quick start from resistant dormant bodies, may significantly affect mediocre functional groups if the minimum bacterial population parameter is set too high.
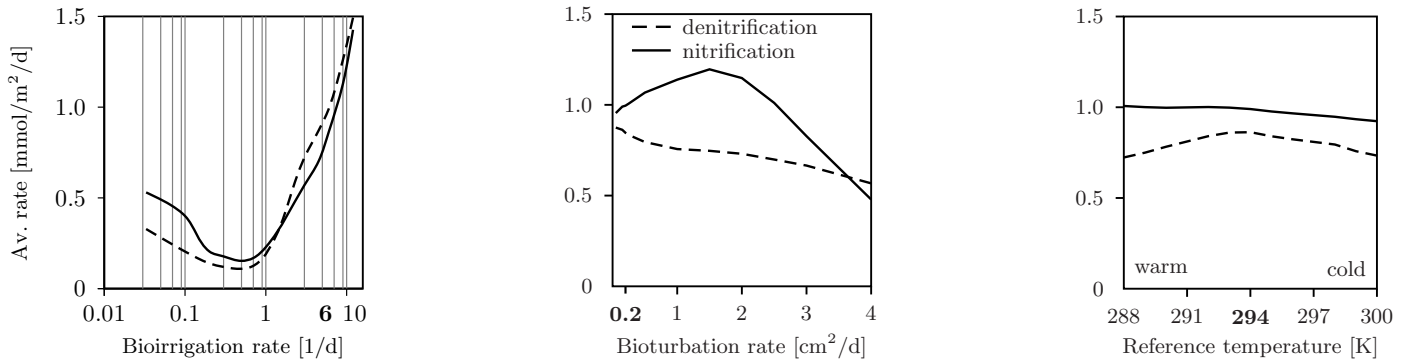
Figure 6: Spatiotemporal averaged nitrification and denitrification rates as a function of bioirrigation rate, β, bioturbation coefficient, D^B, and reference temperature, T_R, for the tidal setup. The standard parameter values are highlighted. Note that an increase in T_R corresponds to a mean temperature decrease of the temperature forcing.
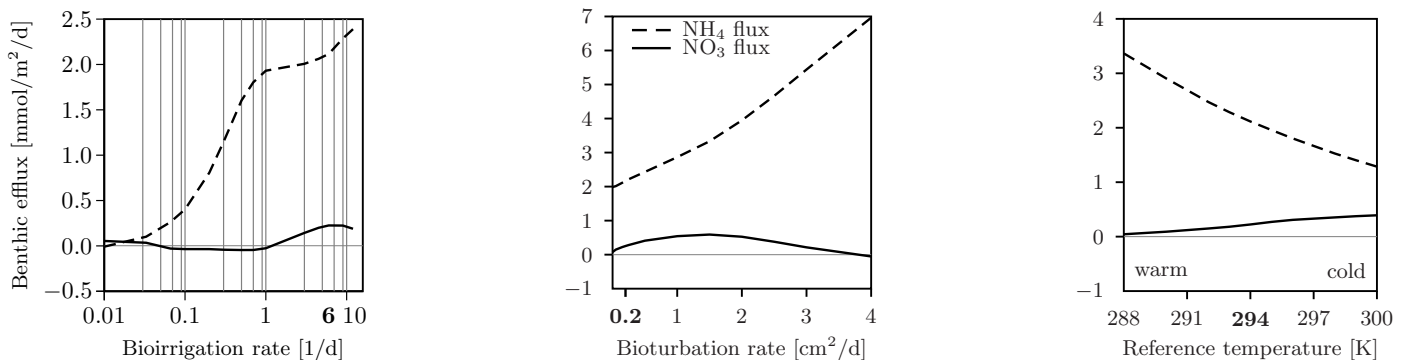

Figure 7: Dependence of mean benthic fluxes of NH_4 and NO_3 on bioirrigation, β, bioturbation coefficient, D^B, and reference temperature, T_R, for the tidal setup. The standard parameter values are highlighted.

Specifically, methanogenesis may be overestimated since outcompeted methanogens are constantly replaced and are able to grow as long as DOC is available. The implementation of minimum bacterial population will therefore be critically reviewed to ensure that biogeochemical cycling is not affected in steady state.

6.1. Inertia of biogeochemical systems

The lower leverages in the deep sea system illustrate the stolid biochemical cycling in such environment. Less steep gradients, broader redox zones, lower temperatures, less reactive OM, and weak forcing increase the inertia of the system, thus resisting changes in single intrinsic or external factors. OM half-life, i.e. POC conversion rates, has a self-amplifying effect through enzymatic decay enhancement: higher bacterial numbers that are supported by enhanced POC decay in return stimulate the POC decay by enzymatic action. For labile POC, such as in the tidal setup, small changes in POC decay, e.g. by seasonal temperature variation, lead to a drastic change in supported population numbers and conversion rates. Therefore, in the tidal setup enzymatic decay enhancement is one of the most influential parameters.

Due to the very low bioturbation and bioirrigation rates in the deep sea setup, exchange of matter across the sediment-water boundary is of much less importance than in the tidal flat setup. Accordingly, parameters for the bottom water concentration generally have a lower impact in the deep sea setup. This applies to the composition of particles in the bottom water as well. As these particles are thought to be in suspension, they are subject to bioirrigation transport just like solutes. Thus, the leverages of bottom water particle composition depend on mixing intensities. This indicates that particles have major impact on the sensitivity of coastal systems, for they represent an important source of both labile OM and metals, as seen in the leverages of POC, Mn^{IV} and Fe^{III} contents.

The differences in model output between the tidal flat and the deep sea setup partly result from the prevalence of different transport modes. Since the main transport mechanism in the deep sea setup is diffusion, the porosity- and diffusion enhancement-related parameters gain relevance, whereas in the tidal flat setup sediment mixing- and bioirrigation related parameters are more influential. When considering the importance of bottom water composition, which is characterized by turbulent mixing and shallowness in coastal ecosystems, the relevance of water column processes for coastal sediments becomes evident. Just like

many pelagic models partially integrate benthic processes [6, 22], a partial integration of water column processes into sediment models appears reasonable in order to further assess water column–sediment feedback mechanisms.

The SA reveals a number of unexpected nonconformities between the setups compared in Fig. 5. Parameters that exhibit divergent sensitivities to certain target variables include the effect of porosity on carbon cycle-specific variables (especially the SWID-OM, CO_2 and CH_4 production), the impact of the fractal dimension of POC on the nitrate flux, the influence of bottom water concentration of nitrate, POC and DOC on nitrate flux, the effect of the aerobic ammonium reduction yield on the nitrogen specific variables, the aerobic methane reoxidation yield on methane flux, and the FeS oxidation rate on NO_3 on nitrification. In some cases, the parameters involved are the calibrated parameters from Tab. 1, such as porosity or bottom water concentrations, or are closely related, such as the fractal dimension of POC relating to POC decay rates. Therefore these divergent sensitivities can be ascribed to model nonlinearities. To clarify the remaining discrepancies further work will need to be done to analyze model behavior that is not *a priori* intelligible in order to discriminate between unexpected interactions and model shortcomings.

6.2. Nitrogen cycling and mixing

Variablilty in bioirrigation and bioturbation may cause different nitrogen dynamics, e.g. shifts from import to export of NO_3. Nitrification and denitrification are alternatively affected in the same or in the opposite way within certain intervals of bioirrigation and bioturbation intensities, as depicted in Fig. 6 and Fig. 7.

In contrast to model formulations, the colonisation density of irrigating organisms controls the dimension of the transition zone between oxic and anoxic environments around burrow structures [1]. The suboxic conditions promote denitrification [24], but according to Gilbert et al. [23] the irrigated sediment zone eventually can become fully aerated when the colonisation density becomes very high resulting in decreased denitrification rates. Due to spatial resolution, the model bioturbation does not account for geometric considerations. Instead, increased bioirrigation simply increases the thickness of the suboxic zone. Kristensen and Blackburn [33], working with polychaetes in microcosm, report stimulated nitrification, denitrification and benthic fluxes through bioturbating organisms, which is not confirmed for denitrification by model results. However, if a bioirrigating effect is also assumed for the organisms, increased denitrification is likely to occur. The effect on biogeochemistry of specific colonisation and activity patterns of organisms is rarely considered in models [36, 37], even though biogenous sediment heterogeneities may have considerable impact on nitrogen cycling [5, 47]. The different responses of nitrification and denitrification to parameter changes lead to strong fluctuations of the ratio of denitrification to nitrification. Denitrification rates

never fall below 68 % of nitrification and seem to be over-estimated compared to literature data [26, 25, 30]. Since the reaction specific energy yield of bacteria is related to the Gibbs free energy of the respective reaction, denitrifiers in the model derive about as much energy from OM reduction as aerobic heterotrophs, which may not be realistic. Certainly, the model ignores that different organisms can influence nitrogen turnover in specific ways [48], which limits the soundness of model results. Macrobenthic biota are not explicitly modeled, although excretion of fecal pellets stimulates ammonium release and nitrification within the pellets [27]. The effect of macroorganisms is incorporated through bioirrigation and bioturbation, but in a static way so that in the model these effects will not react to habitat changes as proposed by Reise [43]. Likewise, the addition of phytobenthic activity would add essential habitat characteristics with considerable effect on benthic nitrogen fluxes. Implications for biogeochemical cycles related to carbon fixation, release of oxygen and polymeric exudates would add a layer of complexity through superposition of day-night and tidal cycles. Food-web effects, such as top-down control of phytobenthos or bacteria by meio- and macrobenthic organisms are also lacking in the model [39, 2]. As it stands, the specific activity patterns of infauna are absolutely important for nitrogen cycling. The physical aspects of bioturbation and bioirrigation, the parameters of biodiffusion, and the extent of non-local transport are highly uncertain for most locations. Their impact on nitrogen cycling, reflected by the heterogeneous sensitivity pattern of the transport and mixing parameter subset, suggests that constraints to bioturbation and bioirrigation activity [20] as well as more detailed model formulations [14, 38] are essential to obtain increasingly realistic model results.

6.3. Linking carbon and nitrogen cycles

The carbon cycle has an overall lower sensitivity to changes in input parameters than the nitrogen cycle; this is not a result of the model construction. There are about as many heterotrophic redox reactions (6) as there are nitrogen-related ones (7), denitrification being part of both groups (cmp. Tab. 2). For nitrogen, a high potential for internal feedback is created by the four denitrifying reactions (anammox and denitrification with Mn, Fe and FeS) and depends on nitrification for nitrate supply and competition with other secondary redox bacteria for electron donors. In contrast, the carbon degrading processes generally interfere less with each other. The high load of labile OM in the tidal setup creates a mode of dominate sulfate reduction, where the generated H_2S effectively scavenges reduced metals, thereby inhibiting the heterotrophic metal oxidizers. Once high H_2S concentrations build up in surface sediments, even aerobic heterotrophs are decreased through the depletion of oxygen by the H_2S oxidation. The dominance and self-amplification of sulfate reducers by suppressing competitors through metabolite restriction inhibits major functional shifts. In the deep sea setup,

the biomass of heterotrophic bacteria is mainly distributed among oxygen and sulfate reducers. Due to scarcity in reducible substances, the remaining heterotrophic functional groups barely survive. This is also reflected by the much smaller sensitivity difference between carbon and nitrogen cycles in the deep sea setup where functional shifts represented by SWID-OM and SWID-NO3 are mainly restricted to changes in POC decay.

Metal cycling is related to both carbon and nitrogen cycling. However, the impact of metal cycling-related parameters generally suggests predominant nitrogen–metal interrelations, not solely because there are 3 metal–nitrogen redox paths and only 2 metal-OM redox paths in the model. The metal–nitrogen redox paths are also preferentially utilized, especially for the parameter subsets: reaction specific energy yield, bottom water concentrations and abiotic reaction coefficients. Here the SA reveals that the nitrogen cycle holds an intermediate position between carbon and metal cycling. Even though the reaction specific energy yield and abiotic reaction parameter leverages are mostly low, they may not be disregarded, since the uncertainty of these parameters is considerable. Apart from metal cycling, carbon and nitrogen cycles appear closely coupled, related to the release of both elements in fixed ratios during biomass degradation. Hence, variations in nitrogen cycling are usually accompanied by changes in CO_2 generation and shifts in heterotrophic pathway partitioning. Exceptions to the coupling are confined to a few process-specific parameters: e.g. the Mn^{II} oxidation yield with NO_3.

No interaction of nitrification and aerobic methane oxidation can be deduced from the SA, although nitrogen limitation of methanotrophs as well as inhibition of nitrifiers by methanotrophs has been reported by [18] in coastal sediments. An interaction between nitrifiers by methanotrophs can be expected, since both compete for oxygen, but the lack of a permanent oxygenated layer in the tidal flat setup makes aerobic methane oxidation insignificant. A leverage of -2 for the NO_3 reduction yield on the benthic CH_4 flux suggests that aerobic methane oxidizers are outcompeted by denitrifers due to their lower energy yield. The relatively high leverage of CH_4 oxidation with SO_4 on benthic CH_4 flux confirms that anaerobic methanotrophs metabolize close to their thermodynamic limit as proposed by Dale et al. [19]

6.4. Sensitivity in terms of parameter leverages

In contrast to classical sensitivity studies, which map the sensitivity according to a fixed parameter change, v, the use of leverage specifies the parameter change needed to obtain a significant reaction in the system. It is therefore suited to estimate the actual impact of parameter uncertainty. Predetermination of v according to an estimative or arbitrary uncertainty of the respective parameter is unnecessary. Since leverage indicates the magnitude of parameter influence, comparison with parameter uncertainty produces its actual impact. In other words, an influential

but well known and invariant parameter may have less importance for a variable than a less influential but unconstrained parameter. Both leverage and uncertainty add up to the relevance of a parameter for model soundness. As uncertainty is not a model feature but is subject to *a posteriori* change, it seems undesirable to use the former to derive v, as suggested by classical sensitivity analysis. Since leverage is calculated from the relative change in v, generating a specific response level, problems that arise from comparing sensitivities that originate from different values of v can be avoided: the resulting leverage matrix allows the comparison of model sensitivities that are valid on very different scales. Occurrences of unrealistic variations, e.g. $v = 2$ for T_R or porosity, are still possible but are confined to those target variables that are obviously insensitive to this parameter. However, the numerical effort of calculating leverage is usually several times higher than that required for a classical SA, depending on v stepping and how sensitivities are distributed. On the other hand, scanning a range of parameter values will also return more complete information on how a specific parameter affects the target variables regardless of parameter uncertainty. The leverage method can easily be extended to calculate the second derivatives of the model in order to better assess nonlinear processes.

7. Conclusions

The leverage approach demonstrates its usefulness in assessing model sensitivity. The separation of parameter leverage and parameter uncertainty appears advantageous as the sensitivity analysis is valid for a calibration regardless of research question or study site. The model demonstrates robustness in the sense of structural stability, as it shows comparable sensitivities regardless of calibration. While temperature and bacterial parameters are important to both analyzed scenarios, the tidal flat setup is characterized by specific sensitivities to not only transport and mixing but also organic matter parameters, especially enzymatic POC decay enhancement, the OM content of particles, and the yield of sulfate reducers on DOC. The number of sensitivities found in a steady state setup implicates a rather small potential for ad-hoc model simplification. In contrast, the deep sea sensitivities are more detached. Although the deep water setup was overall less sensitive to changes in the input parameters, parameters such as the temperature susceptibility of bacterial metabolism, the oxygen content of the bottom water, and the sediment porosity are on par with the overall higher sensitivity of the tidal flat setup. The different effects between the setups and the higher significance of bioirrigation and bioturbation to the tidal flat demand further investigations. These should broaden the empirical bases of estimates for habitat specific bioirrigation and bioturbation coefficients related to macrobenthic activity and may identify possible commonalities between these parameters.

The general high sensitivity of the nitrogen cycle to parameter changes emphasizes the need for sophisticated models specifically engaging the nitrogen cycle in order to characterize terms and conditions on which sediments act as sinks or sources for NO_3, the influence of specific irrigation and mixing habits of macrobenthic communities, and the implications for N_2O generation. The extension of leverage to classical sensitivity analyses will add to the array of tools available for assessing the impact of parameter change and uncertainty of complex systems. Though numerically more demanding, it accounts for parameter uncertainty and considers not only nonlinear system behavior but also different parameter scales.

Appendix. Model principles

A.1. Transport

Transport processes are divided into non-local transport of solutes (bioirrigation) and local transport processes of solutes and solids, i.e. diffusion, bioturbation, advection and sedimentation. The effective diffusion coefficient, D_i, is a composite of molecular diffusion and mixing due to bioturbation:

$$D_i = \frac{D^{sw}}{\theta^2} + D_z^B \qquad (A1)$$

The temperature sensitive diffusion coefficient of dissolved chemical species D^{sw} is taken from a comprehensive literature study [15] and linearly depends on temperature. Diffusive transport between two neighboring model boxes is calculated according to a relaxation scheme using effective box volumes in the vicinity of the respective border. For small box sizes, the solution converges to Fick's second law of diffusion. Bioturbation is scaled by the depth dependent biodiffusion coefficient D_z^B and allows intraphase mixing only. Bioirrigation is implemented as non-local transport connecting every sediment box directly to the bottom water with pelagic matter concentrations $C_{0,i}$. Hence, for any concentration of biochemical species i, the relaxation scheme reads

$$\dot{C}_i = \beta_z \cdot (C_{0,i} - C_i) \qquad (A2)$$

In order to account for fading mixing in deeper sediment layers, D_z^B and β_z exponentially decrease with depth and vanish at bioturbation depth z_B and bioirrigation depth z_β, respectively. At $z = 0$, D_z^B and β_z equal the biodiffusion coefficient D^B and bioirrigation coefficient β. Porosity ϕ and tortuosity θ are characteristic for each box and, thus, not transported. In order to account for stratification, lateral facies zonation, or inhomogeneous permeabilities, the exponential porosity decreases after Rabouille et al. [42] and the calculation of tortuosity from porosity using Boudreau's law [15] may be overridden, allowing predefinition of porosity and tortuosity for each box. Sedimentation/erosion acts like advection; however, it affects both solids and solutes in the same way.

A.2. Geochemical Reactions

The geochemical module comprises four types of reactions: (i) Hydrolysis of particulate organic matter (represented by POC) to dissolved organic matter (DOC) in classes of different quality, (ii) fermentation and oxidation of high molecular weight organic carbon HM-DOC and oxidation of low molecular organic carbon LM-DOC, (iii) reoxidation of reduced species and (iv) mineral precipitation. The reactions are summarized in Tab. 2. The organic matter degradation module is based on the model presented by Boudreau [13]. Global POC, HM-DOC and LM-DOC pools are subdivided into three fractions each, defined according to turnover time and Redfield ratios, reflecting different inherent qualities, origin and degree of decomposition. Since the use of hydrolytic exoenzymes belongs to the disposal of bacterial foraging strategies, POC hydrolysis is enhanced by aerobic bacteria [52, 12]. As only fermentation converts HM-DOC into LM-DOC, the distribution ratio of POC to the DOC-pools may create a fermentation bottleneck for subsequent mineralization processes.

Nitrogen dynamics have an explicit link to the carbon cycle by ammonification of the POC classes. Also, denitrifiers compete with other heterotrophs for OM and with metal oxidizing lithotrophs for nitrate. Lastly, two types of anaerobic ammonium oxidizers, nitrate and manganese reducers, compete for ammonium. With interrelations to carbon as well as metal cycling, seven nitrogen reactions allow the display of a comprehensive spectrum of nitrogen dynamics under oxic, suboxic and anoxic conditions.

NH_4 and PO^{+4} are subject to adsorption, so that they exist in both solid and aqueous phases at concentrations C_s and C_{aq}, respectively. Adsorption is implemented as first order Freundlich Isotherm, i.e.

$$\frac{C_s}{C_{aq}^l} = \mathcal{K}_{ad} \qquad l = 1 \qquad (A3)$$

with $\mathcal{K}_{ad}$ being the adsorbtion constant and l the Freundlich exponent.

Monosulfide precipitation (reactions R-23 and R-24 as defined in Tab. 2) is assumed to be in thermodynamic equilibrium according to the law of mass action. With Me as a placeholder for the metals iron or manganese we have

$$[Me] \cdot [H_2S] = \vartheta(T) \cdot \mathcal{K}_{eq} \qquad (A4)$$

where $\mathcal{K}_{eq}$ is the equilibrium constant for the respective reaction at reference temperature and $\vartheta(T)$ a nonlinear temperature term (see A.4) accounting for the fact that the equilibrium of endothermal reactions (e.g. metalsulfide dissolution) is shifted towards the products at higher temperatures.

Reoxidation of monosulfides and pyrite formation (reactions R-25–R-29) are rate controlled reactions. The temperature sensitive reaction rate R_n

$$R_n = r_n \cdot \vartheta(T) \cdot L_n \quad \text{with } L_n = a \cdot \begin{cases} b/b_{lim} & : \quad \text{if } b < b_{lim} \\ 1 & : \quad \text{else} \end{cases}$$

Table 2: Diagenetic reactions resolved within the model. Organic material is chemically represented by carbohydrate CH_2O.

Hydrolysis of particulate organic matter classes with variable C:N:P:Si ratios	
$(CH_2O)_c(NH_3)_n(H_3PO_4)_p(H_4SiO_4)_s \rightarrow c(CH_2O) + n(NH_3) + p(H_3PO_4) + s(H_4SiO_4)$	R-0[†]
fermentation of high molecular (HM) to low molecular (LM) organic matter	
$CH_2O\,(HM) \rightarrow CH_2O\,(LM)$	R-1[†]
Primary redox reactions and adsorption	
$CH_2O + O_2 \rightarrow CO_2 + H_2O$	R-10[†]
$CH_2O + \frac{4}{5}NO_3^- \rightarrow \frac{2}{5}N_2 + \frac{1}{5}CO_2 + \frac{4}{5}HCO_3^- + \frac{3}{5}H_2O$	R-11[†]
$CH_2O + 2MnO_2 + 3CO_2 \rightarrow 2Mn^{2+} + 4HCO_3^-$	R-12[†]
$CH_2O + 4Fe(OH)_3 + 7CO_2 \rightarrow 4Fe^{2+} + 8HCO_3^- + 3H_2O$	R-13[†]
$CH_2O + \frac{1}{2}SO_4^{2-} \rightarrow \frac{1}{2}H_2S + HCO_3^-$	R-14[†]
$CH_2O \rightarrow \frac{1}{2}CH_4 + \frac{1}{2}CO_2$	R-15[†]
$NH_4^+ + 2O_2 + 2HCO_3^- \rightarrow NO_3^- + 2CO_2 + 3H_2O$	R-16[‡]
$NH_4^+ + \frac{3}{5}NO_3^- + \frac{2}{5}HCO_3^- \rightarrow \frac{8}{5}N_2 + \frac{2}{5}CO_2 + \frac{11}{5}H_2O$	R-17[†]
$NH_4^+ + \frac{3}{2}MnO_2 + 3CO_2 \rightarrow \frac{1}{2}N_2 + \frac{3}{2}Mn^{2+} + \frac{1}{2}H_2 + 3HCO_3^-$	R-18[†]
$NH_4^+ \leftrightarrow NH_{4,ads}^+$	R-19
$PO_4^+ \leftrightarrow PO_{4,ads}^+$	R-20
Secondary redox reactions	
$Mn^{2+} + \frac{1}{2}O_2 + 2HCO_3^- \rightarrow MnO_2 + 2CO_2 + H_2O$	R-30[†]
$Mn^{2+} + \frac{2}{5}NO_3^- + \frac{7}{5}HCO_3^- + \frac{1}{10}H_2 \rightarrow MnO_2 + \frac{1}{5}N_2 + \frac{7}{5}CO_2 + \frac{3}{5}H_2O$	R-31[†]
$Fe^{2+} + \frac{1}{4}O_2 + 2HCO_3^- + \frac{1}{2}H_2O \rightarrow Fe(OH)_3 + 2CO_2$	R-32[†]
$Fe^{2+} + \frac{1}{5}NO_3^- + \frac{1}{5}HCO_3^+ + \frac{14}{5}H_2O \rightarrow Fe(OH)_3 + \frac{1}{10}N_2 + \frac{1}{5}CO_2$	R-33[†]
$Fe^{2+} + \frac{1}{2}MnO_2 + HCO_3^- + 2H_2 \rightarrow Fe(OH)_3 + \frac{1}{2}Mn^{2+} + H_2O$	R-34[†]
$H_2S + 2O_2 + 2HCO_3^- \rightarrow SO_4^{2-} + 2CO_2 + 2H_2O$	R-35[†]
$H_2S + MnO_2 + 2CO_2 + 4H_2O \rightarrow Mn^{2+} + H_2SO_4 + 2HCO_3^- + 3H_2$	R-36[†]
$H_2S + 2Fe(OH)_3 + 4CO_2 + 2H_2O \rightarrow 2Fe^{2+} + H_2SO_4 + 4HCO_3^- + 6H_2$	R-37[†]
$CH_4 + 2O_2 \rightarrow CO_2 + 2H_2O$	R-38[†]
$CH_4 + SO_4^{2-} \rightarrow CO_3^{2-} + H_2S + H_2O$	R-39[†]
Monosulfide precipitation, reoxidation and pyrite formation	
$Mn^{2+} + 2HCO_3^- + H_2S \leftrightarrow MnS + 2CO_2 + 2H_2O$	R-50
$Fe^{2+} + 2HCO_3^- + H_2S \leftrightarrow FeS + 2CO_2 + 2H_2O$	R-51
$MnS + \frac{5}{2}O_2 + 2HCO_3^- \rightarrow MnO_2 + SO_4^{2-} + H_2O + 2CO_2$	R-52
$FeS + \frac{9}{4}O_2 + 2HCO_3^- + \frac{1}{2}H_2O \rightarrow Fe(OH)_3 + SO_4^{2-} + 2CO_2$	R-53
$FeS + \frac{9}{5}NO_3^- + \frac{1}{5}HCO_3^- + \frac{7}{5}H_2O \rightarrow Fe(OH)_3 + SO_4^{2-} + \frac{9}{10}N_2 + \frac{1}{5}CO_2$	R-54
$FeS + \frac{9}{2}MnO_2 + 7CO_2 + 5H_2O \rightarrow Fe(OH)_3 + SO_4^{2-} + \frac{9}{2}Mn^{2+} + 7HCO_3^-$	R-55
$FeS + H_2S \rightarrow FeS_2 + H_2$	R-56

[†] Reaction is processed by bacteria

depends on the specific rate constant r_n and the limitation term L_n. While linear to electron donor concentrations a, the reaction kinetics is shifted from second to first order if the electron acceptors concentration b exceeds a certain saturation concentration b_{lim}.

A.3. Rate limitation by bacterial activity

The major part of the reactions (R-1–R-18; R-30–R-39), fermentation and oxidation of organic carbon and reoxidation, are controlled by the catabolic substrate turnover of bacteria. In the model, each population of bacteria represents a functional group defined according to its metabolic pathway. The reaction rates R_n (n=R-1, $\cdots$, R-18, R-30, $\cdots$, R39) are linear functions of the active biomass $X_{act,n}$ of the respective microbial population. Again, we employ an electron acceptor-controlled second to first order reaction kinetic shift analogous to Eq. A5,

$$R_n(X_{act,n}) = r_g \cdot \vartheta(T) \cdot L_n \cdot X_{act,n} \qquad (A6)$$

where r_g is a global rate constant.
In summary, energetically less favorable pathways are not directly inhibited but can be limited by decreased activities of outcompeted microbial populations.

A.4. Activation energy

Activation energy of chemical reactions is implicitly resolved by the temperature coefficient $\mathcal{Q}_{10}$. It controls the temperature dependence ϑ of reaction and growth rates, i.e.

$$\vartheta(T) = \mathcal{Q}_{10}^{1/10}(T - T_R) \qquad (A7)$$

T and T_R are ambient and reference temperature in Kelvin. For simplicity, all chemical and biological temperature dependencies use the same value of $\mathcal{Q}_{10}$.

A.5. Microbial population dynamics

A.5.1. Population growth

The microbial growth module essentially resembles Malthus' theory of population growth [34]. It also includes density regulation, where the reproductive rate depends on the population size and a measure for the carrying capacity X_{cap}, which among others factors, represents spatial limitations. Moreover, only active bacteria with concentration X_{act} take part in reproduction whereas dormant bacteria (X_{dorm}) have their mortality lowered by the factor δ:

$$\dot{X}_n = gX_{act,n} - \rho(X_{act,n} + \delta X_{dorm,n})$$
$$\text{with} \quad g = y_n \cdot \sigma \cdot r_g \cdot \vartheta(T) \cdot L_n \cdot \frac{X_{cap}}{X_n + X_{cap}} \quad \text{and} \quad \rho = m \cdot \vartheta(T)$$
$$(A8)$$

y_n is the reaction specific energy yield which determines how much energy the functional group n can convert into biomass from the energy gain released by catabolic reaction R_n ; σ denotes an ubiquitous growth coefficient and

m is the mortality. The temperature dependent loss term ρ comprises both respiration and mortality e.g. by grazing. Aside from the metabolic pathway, the functional groups solely differ in the specific energy yield of the reaction employed. In the model we assume all reactions to be catabolic, i.e. there is no assimilation of carbon or any other nutrient by the bacteria, thus bacteria do not represent a pool for chemical species. Therefore, organic carbon is immediately and completely converted to CO_2 upon bacterial use.

A.5.2. Dormancy

Adaptive processes within each functional group are restricted to behavioral aspects on the level of individual cells such as dormancy and motility. The concept of dormancy as already introduced by [56] was upgraded from extreme value switching to continuous behavior. It is a simple analogy to theoretical considerations made by Boudreau [16] and refers to the general observation that organisms replicate only when conditions are beneficial. If not, they concentrate on survival through environmental stresses. The fraction of active, i.e. non-dormant biomass is expressed by α

$$X_{act} = \alpha X \qquad \text{where } 0 < \alpha < 1 \qquad (A9)$$

Substituting Eq. A8 with Eq. A9 gives

$$\dot{X} = \hat{r}X = \Big(\alpha \cdot [g - \rho\,(1-\delta)] - \rho\delta\Big)X \qquad (A10)$$

Changes in α reflect bacterial adaptation to changing environmental conditions. Based on the Adaptive Dynamics approach for phenotypic traits proposed by [56], bacteria embark on a strategy of maximizing the growth rate, i.e.

$$\dot{\alpha} := \alpha\,(1-\alpha)\,\frac{\partial \hat{r}}{\partial \alpha} \qquad (A11)$$

Adaptive changes will, thus, be rather slow at extreme values of α and fast at intermediate values and large growth benefits.

[1] Aller, R. C., 1994. Bioturbation and remineralization of sedimentary organic-matter - effects of redox oscillation. Chemical Geology 114, 331–345.

[2] An, S., Joye, S. B., 2001. Enhancement of coupled nitrification-denitrification by benthic photosynthesis in shallow estuarine sediments. Limnology and Oceanography 46, 62–74.

[3] Andersson, J. H., Middelburg, J. J., Soetaert, K., 2006. Identifiability and uncertainty analysis of bio-irrigation rates. Journal Of Marine Research 64, 407–429.

[4] Arzayus, K. M., Canuel, E. A., 2005. Organic matter degradation in sediments of the york river estuary: Effects of biological vs. physical mixing. Geochimica et Cosmochimica Acta 69, 455–464.

[5] Asmus, R. M., Jensen, M. H., Jensen, K. M., Kristensen, E., Asmus, H., Wille, A., 1998. The role of water movement and spatial scaling for measurement of dissolved inorganic nitrogen fluxes in intertidal sediments. Estuarine Coastal and Shelf Science 46, 221–232.

[6] Baretta, J. W., Ebenhöh, W., Ruardij, P., 1995. The european-regional-seas-ecosystem-model, a complex marine ecosystem model. Netherlands Journal of Sea Research 33, 233–246.

[7] Beck, M., Dellwig, O., Holstein, J. M., Grunwald, M., Liebezeit, G., Schnetger, B., Brumsack, H.-J., 2008. Sulphate, dissolved organic carbon, nutrients and terminal metabolic products in deep pore waters of an intertidal flat. Biogeochemistry 89, 221–238.

[8] Beck, M., Köster, J., Engelen, B., Holstein, J. M., Gittel, A., Könneke, M., Riedel, T., Wirtz, K., Cypionka, H., Rullkötter, J., Brumsack, H.-J., 2008. Deep pore water profiles reflect enhanced microbial activity towards tidal flat margins. Ocean Dynamics 59, 371–383.

[9] Begon, M., Harper, J. T., Townsend, C. R., 1990. Ecology: Individuals, Populations and Communities. Blackwell Scientific, Boston, MA.

[10] Berg, P., Rysgaard, S., Funch, P., Sejr, M. K., 2001. Effect of bioturbation on solutes and solids in marine sediments. Aquatic Microbial Ecology 26, 81–94.

[11] Berg, P., Rysgaard, S., Thamdrup, B., 2003. Dynamic modeling of early diagenesis and nutrient cycling. a case study in an arctic marine sediment. American Journal Of Science 303, 905–955.

[12] Bidle, K. D., Azam, F., 1999. Accelerated dissolution of diatom silica by marine bacterial assemblages. Nature 397, 508–512.

[13] Boudreau, B. P., 1992. A kinetic model for microbic organic-matter decomposition in marine sediments. Aquatic Microbial Ecology 102, 1–14.

[14] Boudreau, B. P., 1994. Is burial velocity a master parameter for bioturbation. Geochimica et Cosmochimica Acta 58, 1243–1249.

[15] Boudreau, B. P., 1997. Diagenetic models and their implementation. Modelling Transport and Reactions in Aquatic Sediments. Springer Verlag, Berlin Heidelberg New York.

[16] Boudreau, B. P., 1999. A theoretical investigation of the organic carbon-microbial biomass relation in muddy sediments. Aquatic Microbial Ecology 17, 181–189.

[17] Brun, R., Kühni, M., Siegrist, H., Gujer, W., Reichert, P., 2002. Practical identifiability of asm2d parameters - systematic selection and tuning of parameter subsets. Water Research 36, 4113–4127.

[18] Carini, S. A., Orcutt, B. N., Joye, S. B., 2003. Interactions between methane oxidation and nitrification in coastal sediments. Geomicrobiology Journal 20, 355–374.

[19] Dale, A. W., Regnier, P., Van Cappellen, P., 2006. Bioenergetic controls on anaerobic oxidation of methane (aom) in coastal marine sediments: A theoretical analysis. American Journal Of Science 306, 246–294.

[20] D'Andrea, A. F., Lopez, G. R., Aller, R. C., 2004. Rapid physical and biological particle mixing on an intertidal sandflat. J. Mar. Res. 62, 67–92.

[21] Dhakar, S. P., Burdige, D. J., 1996. Coupled, non-linear, steady state model for early diagenetic processes in pelagic sediments. American Journal of Science 296, 296–330.

[22] Ebenhöh, W., Kohlmeier, C., Radford, P. J., 1995. The benthic biological submodel in the european-regional-seas-ecosystem-model. Netherlands Journal of Sea Research 33, 423–452.

[23] Gilbert, F., Aller, R. C., Hulth, S., 2003. The influence of macrofaunal burrow spacing and diffusive scaling on sedimentary nitrification and denitrification: An experimental simulation and model approach. Journal Of Marine Research 61, 101–125.

[24] Gruber, N., Sarmiento, J. L., 1997. Global patterns of marine nitrogen fixation and denitrification. Glob. Biogeochem. Cycle 11, 235–266.

[25] Hammond, D. E., Fuller, C., Harmon, D., Hartman, B., Korosec, M., Miller, L. G., Rea, R., Warren, S., Berelson, W., Hager, S. W., 1985. Benthic fluxes in san-francisco bay. Hydrobiologia 129, 69–90.

[26] Henriksen, K., Hansen, J. I., Blackburn, T. H., 1981. Rates of nitrification, distribution of nitrifying bacteria, and nitrate fluxes in different types of sediment from danish waters. Marine Biology 61, 299–304.

[27] Henriksen, K., Rasmussen, M. B., Jensen, A., 1983. Effect of bioturbation on microbial nitrogen transformations in the sediment and fluxes of ammonium and nitrate to the overlaying water. Ecological Bulletins , 193–205.

[28] Holmberg, A., 1982. On the practical identifiability of microbial-growth models incorporating michaelis-menten type nonlinearities. Mathematical Biosciences 62, 23–43.

[29] Holstein, J. M., 2008. Model evidence for the relevance of rapid sedimentation for the biogeochemistry in a tidal flat. in prep. .

[30] Jensen, M. H., Lomstein, E., Sorensen, J., 1990. Benthic nh4+ and no3- flux following sedimentation of a spring phytoplankton bloom in aarhus bight, denmark. Marine Ecology-Progress Series 61, 87–96.

[31] Kelly-Gerreyn, B. A., Hydes, D. J., Waniek, J. J., 2005. Control of the diffusive boundary layer on benthic fluxes: a model study. Marine Ecology-Progress Series 292, 61–74.

[32] Klepper, O., vanderTol, M., Scholten, H., Herman, P., 1994. SMOES: a simulation model for the Oosterschelde ecosystem - Part I: Description and uncertainty analysis. Hydrobiologia 282/283, 437–451.

[33] Kristensen, E., Blackburn, T. H., 1987. The fate of organic-carbon and nitrogen in experimental marine sediment systems - influence of bioturbation and anoxia. Journal Of Marine Research 45, 231–257.

[34] Malthus, T. B., 1798. First essay on population. (Reprinted 1926 Macmillan London).

[35] Meile, C., Koretsky, C., Van Cappellen, P., 2001. Quantifying bioirrigation in aquatic sediments: An inverse modeling approach. Limnology and Oceanography 46, 164–177.

[36] Meile, C., Tuncay, K., Van Cappellen, P., 2003. Explicit representation of spatial heterogeneity in reactive transport models: application to bioirrigated sediments. Journal of Geochemical Exploration 78-9, 231–234.

[37] Meysman, F. J. R., Galaktionov, E. S., Middelburg, J. J., 2005. Irrigation patterns in permeable sediments induced by burrow ventilation: a case study of arenicola marina. Marine Ecology-Progress Series 303, 195–212.

[38] Meysman, F. J. R., Malyuga, V. S., Boudreau, B. P., Middelburg, J. J., 2007. The influence of porosity gradients on mixing coefficients in sediments. Geochimica et Cosmochimica Acta 71, 961–973.

[39] Middelburg, J. J., Barranguet, C., Boschker, H. T. S., Herman, P. M. J., Moens, T., Heip, C. H. R., 2000. The fate of intertidal microphytobenthos carbon: An in situ c-13-labeling study. Limnology and Oceanography 45, 1224–1234.

[40] Middelburg, J. J., Klaver, G., Nieuwenhuize, J., Wielemaker, A., deHaas, W., Vlug, T., vanderNat, J. F. W. A., 1996. Organic matter mineralization in intertidal sediments along an estuarine gradient. Marine Ecology-Progress Series 132, 157–168.

[41] Peng, J., Zeng, E. Y., 2007. An integrated gechemical and hydrodynamic model for tidal coastal environments. Marine Chemistry 103, 15–29.

[42] Rabouille, C., Gaillard, J.-F., Tréguer, P., Vincendeau, M.-A., 1997. Biogenic silica recycling in surficial sediments across the Polar Front of the Southern Ocean (Indian Sector). Deep-Sea Research Part I-Oceanographic Research Papers 44, 1151–1176.

[43] Reise, K., 2002. Sediment mediated species interactions in coastal waters. Journal of Sea Research 48, 127–141.

[44] Schulz, H. D., cruise participants, 1999. Report and preliminary results of Meteor cruise M 46/2, Recife-Montevideo, 12/02/1999 - 12/29/1999. Berichte aus dem Fachbereich Geowissenschaften der Universität Bremen 174, 117pp.

[45] Snowling, S. D., Kramer, J. R., 2001. Evaluating modelling uncertainty for model selection. Ecological Modelling 138, 17–30.

[46] Soetaert, K., Herman, P. M. J., Middelburg, J. J., 1996. A model of early diagenetic processes from the shelf to abyssal depths. Geochimica et Cosmochimica Acta 60, 1019–1040.

[47] Stief, P., de Beer, D., 2006. Probing the microenvironment of freshwater sediment macrofauna: Implications of deposit-feeding and bioirrigation for nitrogen cycling. Limnology and Oceanography 51, 2538–2548.

[48] Svensson, J., Leonardson, L., 1996. Effects of bioturbation by tube-dwelling chironomid larvae on oxygen uptake and denitrification in eutrophic lake sediments. Freshwater Biology 35, 289?300.

[49] Thullner, M., Van Cappellen, P., Regnier, P., 2005. Modeling the impact of microbial activity on redox dynamics in porous media. Geochimica et Cosmochimica Acta 69, 5005–5019.

[50] Tromp, T. K., VanCappellen, P., Key, R. M., 1995. A global-model for the early diagenesis of organic-carbon and organic phosphorus in marine-sediments. Geochimica et Cosmochimica Acta 59, 1259–1284.

[51] Turchin, P., 2003. Complex population dynamics. Princeton University Press, New Jersey.

[52] Vetter, Y. A., Deming, J. W., Jumars, P. A., Krieger-Brockett, B. B., 1998. A predictive model of bacterial foraging by means of freely released extracellular enzymes. Microbial Ecology 36, 75–92.

[53] Wang, Y. F., Van Cappellen, P., 1996. A multicomponent reactive transport model of early diagenesis: Application to redox cycling in coastal marine sediments. Geochimica et Cosmochimica Acta 60, 2993–3014.

[54] Wijsman, J. W. M., Herman, P. M. J., Middelburg, J. J., Soetaert, K., 2002. A model for early diagenetic processes in sediments of the continental shelf of the black sea. Estuarine Coastal and Shelf Science 54, 403–421.

[55] Wilms, R., Sass, H., Köpke, B., Köster, J., Cypionka, H., Engelen, B., 2006. Specific bacterial, archaeal, and eukaryotic communities in tidal-flat sediments along a vertical profile of several meters. Applied and Environmental Microbiology 72(4), 2756–2764.

[56] Wirtz, K., 2003. Control of biochemical cycling by mobility and metabolic strategies of microbes in the sediments: an integrated model study. Fems Microbiology Ecology 46, 295–306.